Chemical Engineering Journal 145 (2008) 211–217

Contents lists available at ScienceDirect

Chemical Engineering Journal

journal homepage: www.elsevier.com/locate/cej

Applicability of the exponential time dependence of flux decline during dead-end ultrafiltration of binary protein solutions

Su-Hsia Lin[a], Chia-Lin Hung[b], Ruey-Shin Juang[b,*]

[a] Department of Chemical Engineering, Nanya Institute of Technology, Chung-Li 320 Taiwan
[b] Department of Chemical Engineering and Materials Science, Yuan Ze University, 135 Yuan-Tung Road, Chung-Li 32003, Taiwan

ARTICLE INFO

Article history:
Received 28 December 2007
Received in revised form 29 February 2008
Accepted 8 April 2008

Keywords:
Protein solutions
Dead-end ultrafiltration
Flux decline modeling
Blocking filtration mechanism

ABSTRACT

Flux decline in the dead-end ultrafiltration (UF) of binary solutions of bovine serum albumin (BSA, p*I* 4.7, MW 67,000) and hemoglobin (Hb, p*I* 7.1, MW 68,000) with polyethersulfone (PES, 100 kDa) and polyacrylonitrile (PAN, 100 kDa) membranes was studied. Key factors affecting the flux decline including solution pH (6.00–7.50), total protein concentration (1.5–9.0 μM), transmembrane pressure (TMP, 10–50 psi), and ionic strength (0.01–0.1 M) were systematically investigated. It was shown that the blocking filtration law could satisfactorily analyze the flux decline behavior. A simplified exponentially time-dependent model was adopted to describe the dynamics of flux decline during UF process, and used to determine the adequate time for membrane cleaning. The mechanism of membrane fouling was also analyzed by blocking filtration law, in which the standard blocking always dominated at the early stage in such UF processes. The fouling mechanism strongly depended on hydrophobic characteristics of the membranes, concentration and charge of the proteins, as well as pH and ionic strength of the solutions.

1. Introduction

The separation or purification of proteins is a crucial process in biotechnological fields due to its wide range of applications in biomedical and food industries. The techniques employed for protein recovery and purification such as chromatography, electrophoresis, and affinity operations have been recently established for producing small quantities of proteins in research laboratories. However, these techniques are relatively difficult to scale-up, which limits production levels [1,2]. Besides, some methods like chromatography and electrophoresis require complex instrumentation support to run efficiently, and usually yield low throughput of the products at an extremely high process cost. Hence, the separation techniques that are able to yield high throughput of the products at a low cost are highly desired in biotechnological industries. Of these potential candidates, ultrafiltration (UF) has ever attracted a considerable amount of attention in recent years for the separation of proteins due to comparatively gentler towards the proteins than separation process on phase changes and more economical than gel chromatography [3–8].

The applications of UF processes are generally limited to the systems where the solutes to be separated have more than 10-fold difference in molecular weight (MW). Molecular size becomes the sole criteria for separation purposes in such cases. However, it is possible to separate proteins and enzymes with comparable MWs by adequately manipulating the parameters such as solution pH, ionic strength, and transmembrane pressure (TMP) [3–5]. For example, van Eijndhoven et al. [4] have indicated the possibility to improve the selectivity of bovine serum albumin (BSA)/hemoglobin (Hb) by reducing salt concentration and adjusting pH to near one of the isoelectric points (p*I*) of Hb. Feins and Sirkar [5] have studied the separation of binary proteins with equivalent MWs using internally staged UF. The fractionation of lysozyme (Ly)/ovalbumin as well as Ly/myoglobin mixtures by 100-kDa hydrophilic polyacrylonitrile membrane was investigated in a vortex flow ultrafilter [9]. Saksena and Zydney [3] have also studied the UF of IgG and BSA with 100- and 300-kDa PS membranes in a stirred cell. Also, the separation of Ly and BSA with Amicon PM 30 membrane and the effect of salt concentration and BSA–Ly interaction on the rate of Ly washout were studied [10].

As mentioned above, the UF of protein mixtures has been studied earlier by manipulating the operating parameters. These studies mostly focused on the enhancement of selectivity rather than the analysis of flux decline phenomena. It is recognized that the main problem restricting practical applications is membrane fouling and the resulting time-dependent flux and rejection behavior [9–12]. Hence, the understanding of fouling mechanism is very important to efficiently perform such UF processes.

Although there are some previous studies of protein filtration that focused on fouling mechanism based on the theoretical

* Corresponding author. Tel.: +886 3 4638800x2555; fax: +886 3 4559373.
E-mail address: rsjuang@ce.yzu.edu.tw (R.-S. Juang).

1385-8947/$ – see front matter © 2008 Elsevier B.V. All rights reserved.
doi:10.1016/j.cej.2008.04.003

Nomenclature

A	effective membrane area (m^2)
B_1	integration constant defined in Eq. (2)
B_2	integration constant defined in Eq. (4)
BSA	bovine serum albumin
C_{tot}	initial (total) protein concentration (μM)
Hb	hemoglobin
J	permeate flux defined in Eq. (14) ($m^3/(m^2\,h)$)
J_0	permeate flux of pure water ($m^3/(m^2\,h)$)
J_F	permeate flux at any time during period 1 ($m^3/(m^2\,h)$)
J_C	permeate flux at any time during period 2 ($m^3/(m^2\,h)$)
k	fluid consistency index defined in Eq. (17) ($((h/m^3)^{1-n}$)
k_1	constant describing the rate of flux decline defined in Eq. (1) (h^{-1})
k_2	constant describing the rate of flux decline defined in Eq. (3) (h^{-1})
MW	molecular weight
n	parameter defined in Eq. (17)
pI	isoelectric point
R^2	correlation coefficient
t	filtration time (h)
t_0	the time at the flux being J_0 (h)
TMP	transmembrane pressure (psi)
V	collective permeate volume (m^3)

Greek letter

α	initial molar concentration ratio of BSA to Hb

approach or mathematical model, there is still considerable controversy regarding the most appropriate fouling mechanism. For example, Hlavacek and Bouchet [13] have reported the well agreement between the experimental data and intermediate blocking model for the pressure rise during a constant flux filtration test. Ho and Zydney [14] have used a combined pore blockage and cake filtration model for BSA successfully describing the fouling behavior during MF. The classical blocking filtration law was still the most one applied to describe the fouling mechanism in filtration processes [15,16]. Besides, there is currently no theoretical model capable of quantitatively describing this transition using a single mathematic expression. An attempt was thus made to give an insight in this topic in this work, in which Hb and BSA were chosen as model proteins and the membranes with a molecular-weight cut-off (MWCO) of 100 kDa were selected. The operating parameters of ionic strength, solution pH, and membrane hydrophobicity were studied in order to analyze the flux decline and fouling mechanism of such UF processes.

2. Flux decline modeling

Let us consider a typical flux curve as a function of time. Lahoussine-Turcaud et al. have suggested that the flux curve can be divided in two domains [17]. Domain 1 corresponds to the initial flux decline at $t \to 0$ and is believed to involve membrane fouling. Domain 2 corresponds to the remaining flux decline $t \gg 0$ and is believed to involve concentration polarization and gel layer formation.

$$J_0 \overset{\text{domain 1, } J_F(k_1)}{\longrightarrow} J_{\infty 1} \overset{\text{domain 2, } J_C(k_2)}{\longrightarrow} J_{\infty 2}$$

Mehta has used a mathematic model to describe the rate of flux decline with time for a given time period: period 1 denotes the initial decline of flux that may be due to the membrane fouling, period 2 corresponds to less severe decrease of flux, and period 3 corresponds to a small decrease of flux [18]. Period 1 (domain 1) corresponds to the initial flux decline that occurs during the early stage of filtration. The rate of flux decline with time is expressed as follows using the model of Mehta [18], i.e.,

$$-\frac{dJ_F}{dt} = k_1(J_F - J_{\infty 1}) \tag{1}$$

Upon integration gives typical flux vs. time curve of membrane filtration:

$$J_F = J_{\infty 1} + B_1 \exp(-k_1 t) \tag{2}$$

where J_F is the flux at any time during period 1, $J_{\infty 1}$ is the flux at the end of period 1, B_1 is an integration constant, k_1 is a constant describing the rate of flux decline that is believed to be associated with membrane fouling, and t is the time. Such an exponential dependence of the flux with time has been practically adopted in UF or MF processes [19–22].

Domain 2 with the same procedure used for domain 1 is described by the difference between the flux at time t in period 2 (J_C) and the flux at the end of period 3 ($J_{\infty 2}$).

$$-\frac{dJ_C}{dt} = k_2(J_C - J_{\infty 2}) \tag{3}$$

and upon integration gives

$$J_C = J_{\infty 2} + B_2 \exp(-k_2 t) \tag{4}$$

where B_2 is an integration constant, k_2 is a constant describing the rate of flux decline which is believed to be associated with concentration polarization and gel layer formation. This model is valid for the periods 2 and 3, that is to say for $t \gg 0$. A $t \approx 0$; the model is not valid.

Monder et al. have proposed a modified model that is a solution for domains 1 and 2 corresponding to the three filtration periods [19]. They matched the solution for $t \to 0$ with the solution for $t \gg 0$ (Eqs. (2) and (4)) using the matching principle proposed by van Dyke [23].

$$\lim_{t\to\infty} J_F = \lim_{t\to 0} J_C \tag{5}$$

This principle is based on the inner limit of the outer solution must match with the outer limit of the inner solution; that is, it is formulated for joining expansions in two neighboring regions [23,24]. Substitution of Eq. (5) to Eqs. (2) and (4) gives:

$$\lim_{t\to\infty}[J_{\infty 1} + B_1 \exp(-k_1 t)] = J_{\infty 1} \tag{6}$$

$$\lim_{t\to 0}[J_{\infty 2} + B_2 \exp(-k_2 t)] = J_{\infty 2} + B_2 \tag{7}$$

The solution, which is uniformly valid over the entire filtration curve, is the composite solution denoted by J and given by [19]:

$$J = J_F + J_C - \lim_{t\to\infty} J_F \tag{8}$$

$$J = B_1 \exp(-k_1 t) + B_2 \exp(-k_2 t) + J_{\infty 2} \tag{9}$$

The constant B_1 can be evaluated with the following initial condition:

$$t \to 0, \quad J = J_0 \tag{10}$$

By combining Eqs. (9) and (10), we obtain:

$$B_1 = J_0 - B_2 - J_{\infty 2} \tag{11}$$

while Eq. (5) gives the following equation for B_2:

$$B_2 = J_{\infty 1} - J_{\infty 2} \quad (12)$$

Substitution of Eqs. (11) and (12) for B_1 and B_2 into Eq. (9) gives

$$J = (J_0 - J_{\infty 1}) \exp(-k_1 t) + (J_{\infty 1} - J_{\infty 2}) \exp(-k_2 t) + J_{\infty 2} \quad (13)$$

This four-parameter exponentially time-dependent expression is essentially valid over the entire filtration flux curve. Here, domain 1 corresponds to intermediate, standard blocking, and domain 2 corresponds to the gel layer or cake layer fouling.

3. Materials and methods

3.1. Reagents and membranes

Hemoglobin (Hb, MW 68,000) and bovine serum albumin (BSA, MW 66,430) were obtained from Sigma Co. The p*I* values for Hb and BSA are 7.1 and 4.9, respectively. The single protein solution was prepared by dissolving protein in 50 mM phosphate buffer, in which the solution pH was controlled in the range 6.0–7.5. The solution was gently agitated for 1 h to ensure homogeneity at 25 °C. Prior to use, the phosphate buffer was filtered through a 0.45-μm Durapore membrane (Millipore, Bedford, MA). The binary protein solution was obtained by mixing single stock solutions with gentle agitation for 20 min, and the solution was also pre-filtered through a 0.45-μm Durapore membrane to remove undissolved proteins and large particulates. The ionic strength of protein solutions was adjusted by the addition of NaCl.

Polyestersulfone (PES) and polyacrylonitrile (PAN) disc membranes used were supplied from Osmonics Co. Both asymmetric membranes had a molecular weight cut-off (MWCO) of 100 kDa. Prior to use, these membranes were soaked overnight in protein solutions to ensure the attainment of equilibrium between the membrane and protein molecules.

3.2. Dead-end UF experiments

Batch UF experiments were performed in a stirred glass cell of 8.0 cm I.D. and 8 cm height (Amicon Model 8400). It had an effective membrane area of 41.8 cm^2 and a cell volume of 400 cm^3. The pressure of stirred cell was applied and controlled by nitrogen gas (TMP = 10–50 psi). The feed (working) volume of the solution was 250 cm^3 and the highest speed of 300 rpm was selected because it could provide effective agitation but prevent the formation of a series vortex in the cell. Experiments were carried out at 25 °C. The solution pH was measured using a pH meter (Horiba F-23, Japan).

The average permeate flux (J) at each run was calculated in the time intervals t_1 and t_2 by

$$J = \frac{V_2 - V_1}{A(t_2 - t_1)} \quad (14)$$

where A is the effective membrane area (m^2) and V is the volume of the permeate (m^3).

The concentrations of binary proteins in the samples were determined using HPLC (Hitachi L-7100) on a Hypersil WP300 column (particle size 5 μm). Two mixtures of 0.1 vol% trifluoroacetic acid in water and 0.1 vol% trifluoroacetic acid in *n*-propanol were used as the mobile-phase gradient. The flow rate was 1 cm^3/min. An aliquot of the sample (10 μL) was injected and analyzed with an UV detector (L-7420) at a wavelength of 280 nm. Each experiment was at least duplicated under identical conditions. The reproducibility of the measurements was within 7% (mostly, 5%).

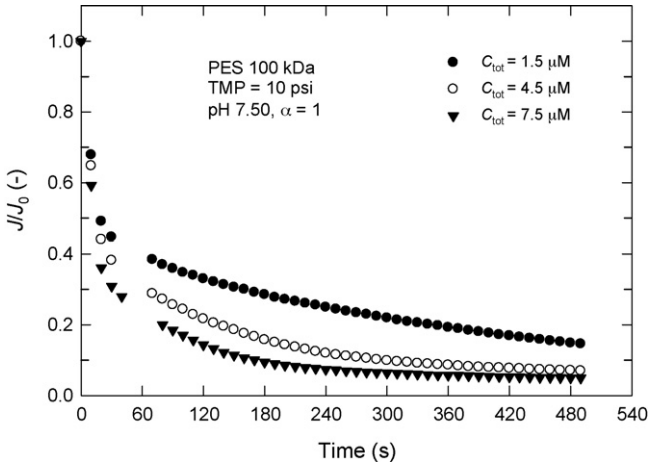

Fig. 1. Variation of J/J_0 as a function of time at a TMP of 10 psi and different pH values during dead-end UF of protein mixtures with PES 100 membrane (J_0 = 54.0 $m^3/(m^2\,h)$).

3.3. Cleaning operations

After the completion of each UF experiment, the membrane used was cleaned in ultrasonic cleaner with 0.1 M NaOH for approximately 30 min once and then with deionized water twice. The pure water flux was then re-checked. The integrity and performance of the membrane was considered to be maintained if pure water flux was within 95% of the virgin membrane. The cleaned membranes were stored in 0.05% sodium azide solution at 4 °C.

4. Result and discussions

4.1. Effects of operating parameters on the flux decline of protein solutions

The effect of membrane materials (PES, PAN) on the UF of equimolar protein mixtures is compared in Figs. 1 and 2. It is evident that the flux decline is more serious with PES membrane under comparable conditions (e.g., pH 7.50, total protein concentration C_{tot} = 1.5–7.5 μM). This is due to the less hydrophilicity of PES membrane than PAN membrane. Consequently, PAN membrane is selected for further studies.

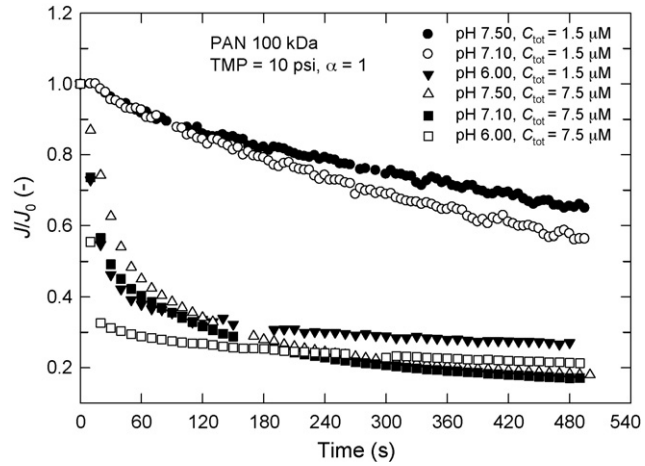

Fig. 2. Variation of J/J_0 as a function of time at a TMP of 10 psi and different pH values during dead-end UF of protein mixtures with PAN 100 membrane (J_0 = 14.4 $m^3/(m^2\,h)$).

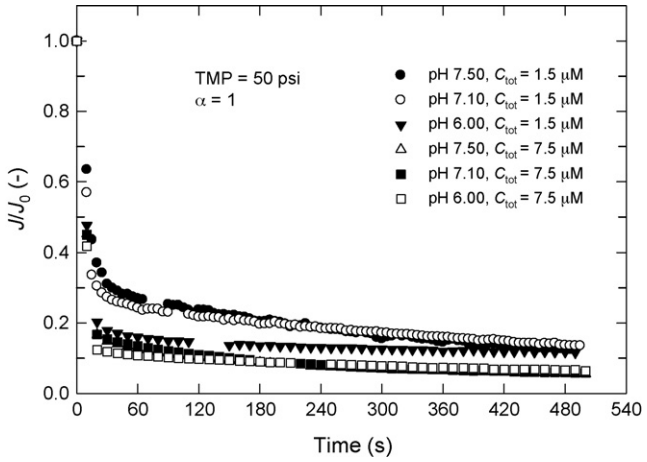

Fig. 3. Variation of J/J_0 as a function of time at a TMP of 50 psi and different pH values during dead-end UF of protein mixtures with PAN 100 membrane (J_0 = 46.8 $m^3/(m^2\,h)$).

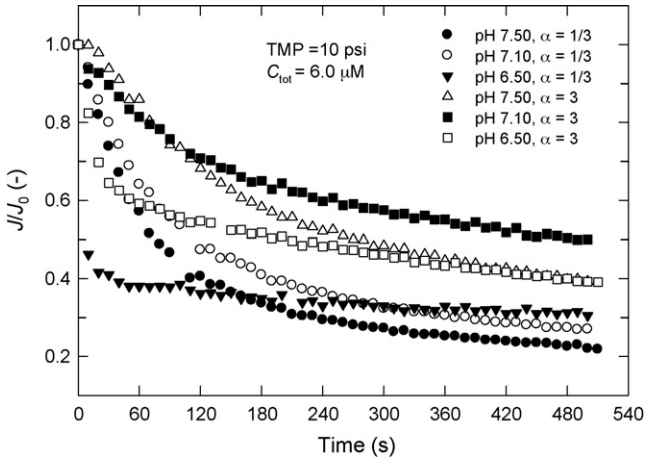

Fig. 5. Variation of J/J_0 as a function of time at a TMP of 10 psi and different protein concentration ratios during dead-end UF of protein mixtures with PAN 100 membrane.

Figs. 2 and 3 show the effect of solution pH and TMP on the flux of binary protein solutions with PAN membranes. It is found that the rate of flux decline is great with time at first and then levels off, particularly at high initial protein concentrations (Fig. 2). It should be noted that the rate of flux decline is small only at the pH of 7.10 (p*I* of Hb protein). However, the effect of solution pH on the flux is more important at low protein concentrations. At pH 6.00, the positively charged Hb would adsorb easily on the negatively charged membrane, and then block the pores of the membrane. Moreover, the repulsive force between the negatively charged proteins and membrane reduces the fouling at pH > 7.10. At higher protein concentration and TMP (Fig. 2), the effect of pH on the flux can be neglected. In such situations, the concentration polarization is more important.

Figs. 4 and 5 show the variations of UF flux as a function of time at various pH values and the initial concentration ratio of BSA to Hb (α). At α = 5, the rate of flux decline decreases with increasing solution pH, but when α = 3 the rate of flux decline displays the smallest value at pH 7.10 under the ranges studied. In comparison with Figs. 4 and 5, it can be seen that the concentration of Hb protein dominates the flux decline. Although the molecular weight of Hb is slightly larger that of BSA, the elliptical shape of Hb would pass easily through the pores of the membrane (equivalent radium in nm: BSA, 14 × 4 × 4; Hb, 7 × 5.5 × 5.5 and ellipsoidal diameter in nm: BSA, 3.61; Hb, 3.10) [15]. The effect of added salt concentration (ionic strength) on the flux is shown in Figs. 6 and 7. It is observed that rate of flux decline decreases with increasing ionic strength. However, this effect is minified at the pH of 6.50. This is because the positively charged Hb (p*I* 7.1) could adsorb on the membrane surface regardless of the ionic strength.

4.2. Dynamic modeling of flux decline

According to the flux decline model described in Section 2, the four parameters of $J_{\infty 1}$, $J_{\infty 2}$, k_1, and k_2 are obtained by fitting Eq. (13) with experimental data. Table 1 shows the best-fitted parameters obtained by SigmaPlot 8.0 version software under different initial protein concentration, solution pH, and TMP with PAN membrane. Here, we use the normalized form of Eq. (13) as follows:

$$\left(\frac{J}{J_0}\right) = \left(1 - \frac{J_{\infty 1}}{J_0}\right) \exp(-k_1 t) + \left(\frac{J_{\infty 1}}{J_0} - \frac{J_{\infty 2}}{J_0}\right) \exp(-k_2 t) + \left(\frac{J_{\infty 2}}{J_0}\right) \quad (15)$$

The calculated flux (J/J_0) vs. time using Eq. (15) coupled with the parameters obtained above are shown in Fig. 8 (pH 7.10, C_{tot} = 9.0 μM, α = 5) and Fig. 9 (pH 6.50, C_{tot} = 9.0 μM, α = 5). Besides the correlation coefficients R^2 given, the standard deviation (S.D.)

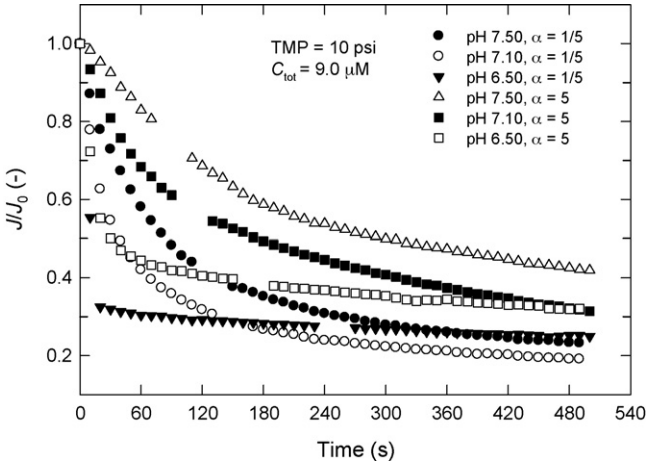

Fig. 4. Variation of J/J_0 as a function of time at a TMP of 10 psi and different protein concentration ratios during dead-end UF of protein mixtures with PAN 100 membrane.

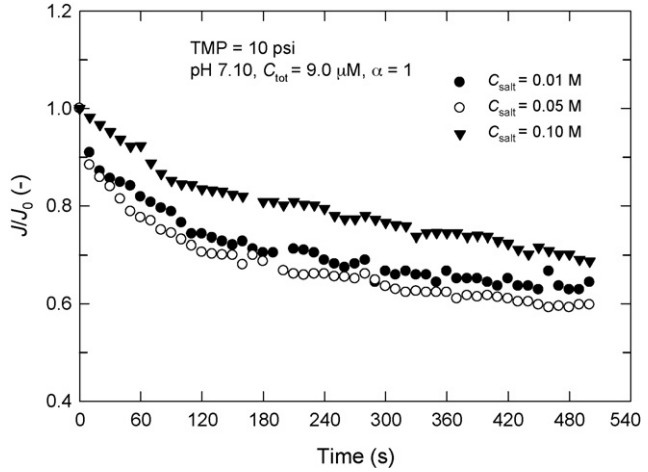

Fig. 6. Effect of ionic strength on the UF flux of protein mixtures with PAN 100 membrane at pH 7.10 and a TMP of 10 psi.

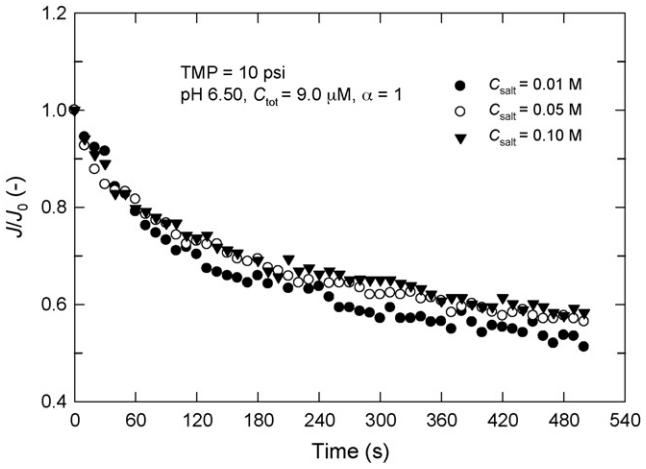

Fig. 7. Effect of ionic strength on the UF flux of protein mixtures with PAN 100 membrane at pH 6.50 and a TMP of 10 psi.

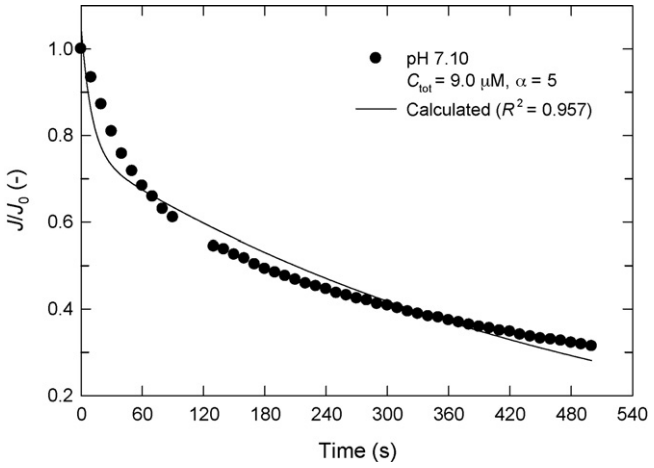

Fig. 8. The calculated and experimental flux decline curves vs. time at pH 7.10 and a TMP of 10 psi with PAN 100 membrane.

between the calculated and experimental data defined in Eq. (16) is obtained to be 8% and 3%, respectively.

$$\text{S.D.}(\%) = \sqrt{\sum \frac{[1 - (J_{calc}/J_{expt})]^2}{(N-1)}} \times 100 \quad (16)$$

where N is the number of data points.

It is evident that the results in Fig. 9 are better predicted than those in Fig. 8. As indicated in Section 2, k_1 is a constant describing the rate of flux decline that is believed to be associated with membrane fouling, and k_2 is considered to be associated with concentration polarization and gel layer formation [19]. As shown in Table 1, the k_1 value increases with increasing TMP when C_{tot} = 1.5 and 7.5 μM at pH 7.1. This reveals that fouling within the pores of the membrane is faster and more serious at higher TMP. However, the k_2 value decreases with increasing TMP, which means that the higher TMP can reduce the resistance of concentration polarization and gel layer. In comparison of pH 6.5 and 7.1 (Table 1) when C_{tot} = 9 μM (α = 5) and 10 psi, both k_1 and k_2 values are lower at pH 7.1 than those at pH 6.5. This is because that the neutral charge of Hb is not easily adsorbed on the surface and within the pores of the membrane.

On the other hand, the larger ratio of (k_1/k_2) reveals better agreement between the measured and modeled data, as shown in the third column from the right side in Table 1. This is likely a result of the more serious flux decline at the early stage of UF process in this situation, which quite matches with the characteristics of the "exponential" decay. The following fouling analysis can support the validity of this argument.

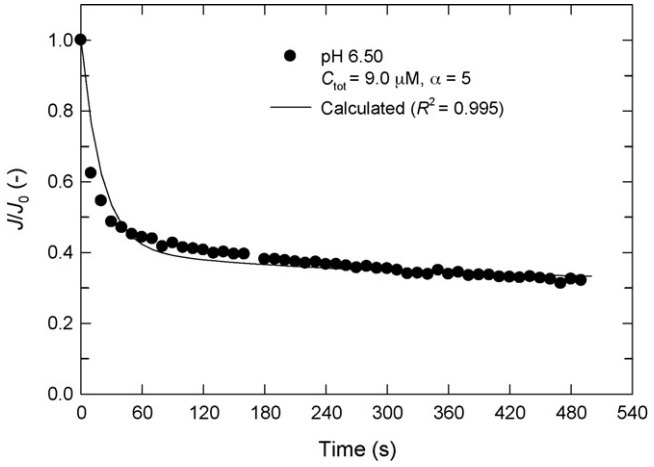

Fig. 9. The calculated and experimental flux decline curves vs. time at pH 6.50 and a TMP of 10 psi with PAN 100 membrane.

4.3. Fouling analysis

In general, the governing equations for fouling mechanism can be described by the so-called blocking filtration law, which is conveniently written in a common mathematical form as [15,16,25,26]:

$$\frac{d^2t}{dV^2} = k\left(\frac{dt}{dV}\right)^n \quad (17)$$

Table 1
Best-fitted model parameters during dead-end UF of binary protein solutions with PAN 100 membrane

C_{tot} (μM)	pH	TMP (psi)	$J_{\infty1}/J_0$ (–)	$J_{\infty2}/J_0$ (–)	k_1 (s^{-1})	k_2 (s^{-1})	k_1/k_2	J_0 ($m^3/(m^2\,h)$)	R^2
1.5 (α = 1)	7.10	10	0.555	–	0.0021	–		14.4	0.978
		20	0.497	0.247	0.0975	0.0033	29.5	23.4	0.942
		30	0.367	0.104	0.163	0.0026	62.7	33.5	0.961
		40	0.311	0.0888	0.186	0.0024	77.5	40.6	0.968
		50	0.270	0.0843	0.194	0.0022	88.2	46.8	0.988
7.5 (α = 1)		10	0.510	0.158	0.0749	0.0066	11.3	14.4	0.953
		20	0.284	0.0902	0.107	0.0058	18.4	23.4	0.950
		30	0.217	0.0681	0.112	0.0052	21.5	33.5	0.958
		40	0.153	0.0461	0.116	0.0042	27.6	40.6	0.962
		50	0.147	0.0401	0.117	0.0037	31.6	46.8	0.982
9.0 (α = 5)	6.50	10	0.412	0.321	0.097	0.0030	32.3	14.4	0.991
	7.10	10	0.363	0.143	0.021	0.0022	9.6	14.4	0.949

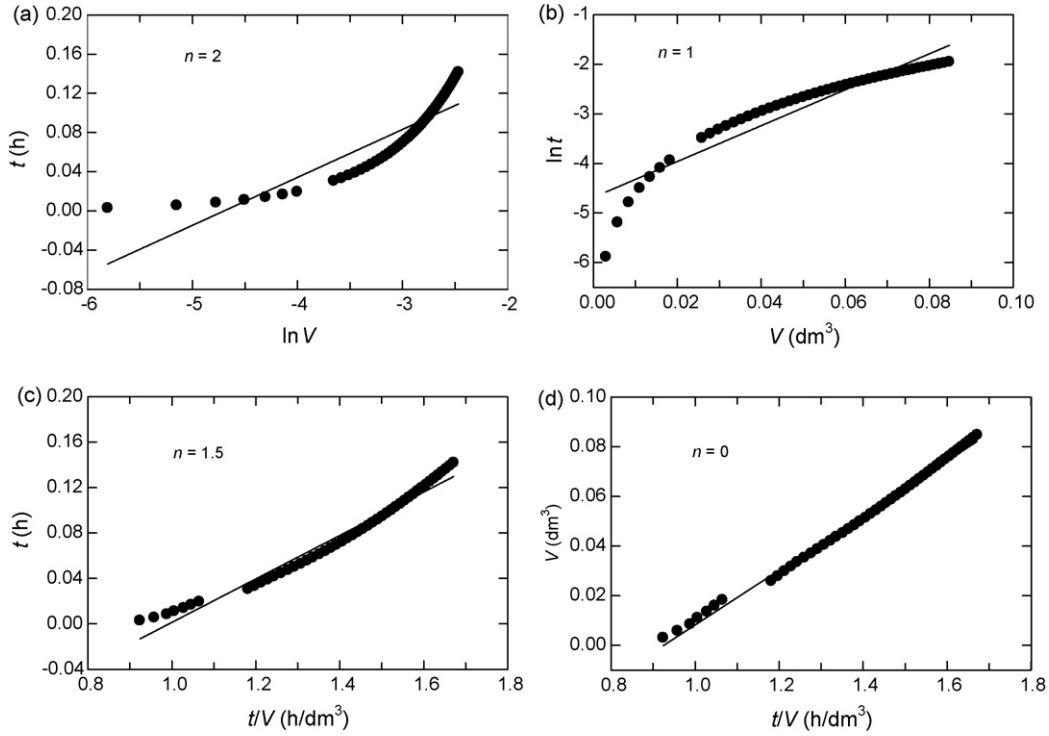

Fig. 10. Blocking filtration analysis during dead-end UF of protein mixtures at pH 7.10 and a TMP of 10 psi (the flux data were taken from Fig. 8).

or,

$$\frac{dJ}{dt} = -kJ(JA)^{2-n} \quad (18)$$

where t is the filtration time (h), V is the collective permeate volume (m^3), J is the flux (=$(1/A)(dV/dt)$), and k is the fluid consistency index ($((h/m^3)^{1-n}$). The exponent n in Eq. (17) characterizes the filtration mechanism, with $n=0$ for cake filtration, $n=1$ for intermediate blocking, $n=1.5$ for standard blocking (also called pore constriction), and $n=2$ for complete pore blocking [16,22,26].

According to Eq. (17), the value of n can be evaluated from the log–log plot of d^2t/dV^2 vs. dt/dV on the flux data. Alternatively, the fitness of each case can be checked by linearly plotting V vs. t/V ($n=0$), V vs. $\ln t$ ($n=1$), t vs. t/V ($n=1.5$), and $\ln V$ vs. t ($n=2$) [12,16]. Figs. 10 and 11 show these results. Table 2 lists the values of n obtained under various conditions. At $\alpha=5$ and pH 7.10 and 7.50, the flux decline with PAN membrane is attributed to the resistance of standard blocking ($n=1.5$) at the early stage and then to that of cake filtration ($n=0$). However, at pH 6.50 flux decline is due to the resistance of complete pore blocking ($n=2$) at the early stage (0–100 s) and gradually to that of intermediate blocking ($n=1$) in the next stage (100–300 s) then changing to that of cake filtration ($n=0$) at the final stage during the period of 300–500 s. The differences of blocking mechanism at the first stage between pH 6.5 and 7.5 are due to the fact that the positive charged Hb is adsorbed preferentially on the surfaces of the membrane and within the pores of the membrane. The pores of the membrane that are adsorbed by Hb may result in the reduction of pore size, leading to the occurrence of complete pore blockage in the first stage at pH 6.5.

On the other hand, the UF behavior of equimolar protein solutions with $C_{tot}=1.5$–7.5 μM at pH 7.50 with PES membrane is considered as the standard blocking ($n=1.5$) at the early stage (0–60 s) and then as the intermediate blocking ($n=1$) in the next stage (60–500 s). However, at pH 7.10 with PES membrane, the flux decline comes from the resistance of standard blocking within 0–90 s, and is then dominated by cake resistance ($n=0$) within 90–500 s. The differences between them are ascribable to the easier aggregation and cake formation for the neutral Hb at pH 7.1 compared to the negative charged Hb at pH 7.5.

The stepwise analysis of blocking filtration law has been ever done by Bowen et al. [16]. They indicated that the flux data at early times yield an exponent of $n=2$ on a plot of d^2t/dV^2 vs. dt/dV, consistent with a pore blockage mechanism. The data at longer times suggest a cake filtration model, with n approaching zero and in some cases attaining a negative value. de Barros et al. [27] have studied the fouling mechanisms in pineapple juice clarification by ceramic tubular UF. They also indicated that complete pore blocking ($n=2$) is the predominant fouling mechanism at the first 10–20 min, after this time that changes to cake fouling. In a word, the filtration mechanism depends on the characteristics

Table 2
The values of n in Eq. (16) during dead-end UF of protein mixtures using PAN and PES membranes (TMP = 10 psi)

Membrane	Feed solution	n value (time range, s)		
PAN 100 kDa	$C_{tot}=9.0$ μM, $\alpha=5$, pH 7.10	1.5 (0–100)	0 (100–500)	–
	$C_{tot}=9.0$ μM, $\alpha=5$, pH 7.50	1.5 (0–100)	0 (100–500)	
	$C_{tot}=9.0$ μM, $\alpha=5$, pH 6.50	2 (0–100)	1 (100–300)	0 (300–500)
PES 100 kDa	$C_{tot}=1.5$–7.5 μM, $\alpha=1$, pH 7.50	1.5 (0–60)	1 (60–500)	–
	$C_{tot}=9.0$ μM, $\alpha=1$, pH 7.50	1.5 (0–60)	1 (60–500)	–
	$C_{tot}=1.5$–7.5 μM, $\alpha=1$, pH 7.10	1.5 (0–90)	0 (90–500)	–

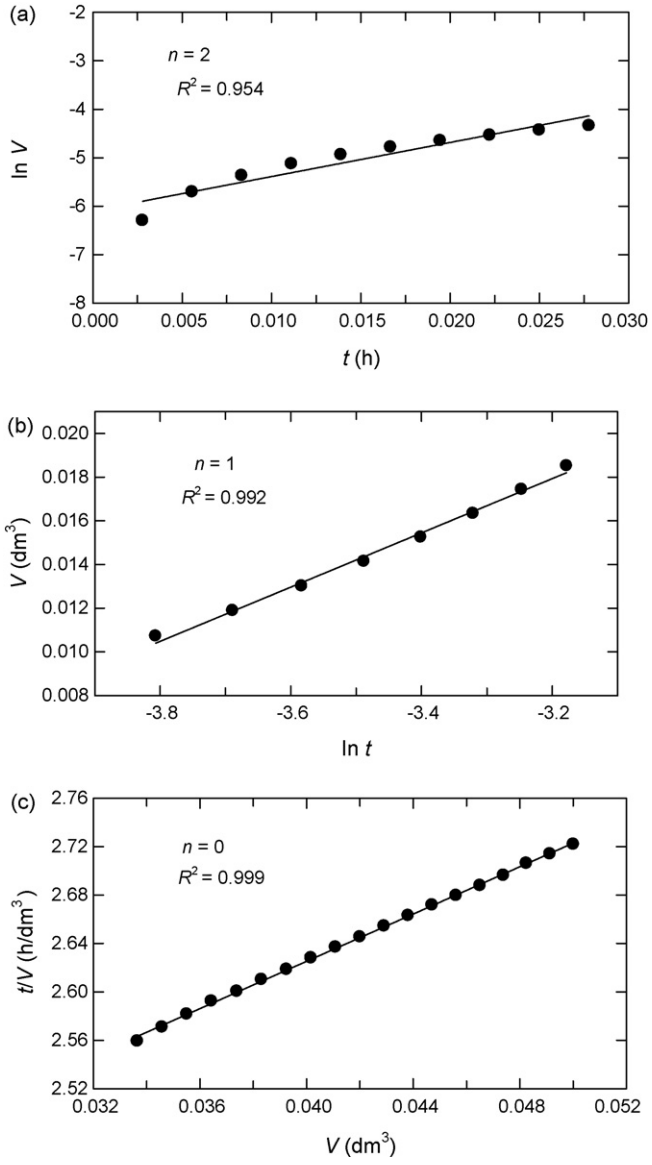

Fig. 11. Blocking filtration analysis during dead-end UF of protein mixtures at pH 6.50 and a TMP of 10 psi (the flux data were taken from Fig. 9).

of the membranes as well as the charge and concentration of the proteins.

5. Conclusions

The effects of operating parameters on flux decline in the dead-end UF of binary bovine serum albumin (BSA) and hemoglobin (Hb) using 100-kDa hydrophilic PAN and hydrophobic PES membranes have been experimentally and theoretically studied. The following results were obtained.

1. Under comparable conditions, the hydrophilic PAN membrane displayed higher UF steady flux than the hydrophobic PES membrane.
2. The higher steady flux was obtained at the solution pH near the higher p*I* of the proteins (in this case, Hb) as well as under the conditions of higher applied pressure and higher ionic strength.
3. The flux decline of UF process was attributed to the standard blocking ($n = 1.5$) and cake filtration at pH larger than the p*I* of Hb with either PAN or PES membrane. However, it was caused by the complete pore blocking in the early stage, and by the intermediate blocking in followed stage and by cake formation at pH 6.50 with PAN membrane.
4. The proposed flux model could satisfactorily describe the dynamics of flux decline when complete pore blocking predominated at the early stage of UF process, which was able to predict the time of membrane cleaning (e.g., backwashing) during the ultrafiltration of protein mixtures.

References

[1] F.T. Sarfert, M.R. Etzel, Mass transfer limitations in protein separations using ion-exchange membranes, J. Chromatogr. A 764 (1997) 3–20.
[2] K. Keller, T. Friedmann, X. Boxman, The bioseparations need for tomorrow, Trends Biotechnol. 19 (2001) 438–441.
[3] S. Saksena, A.L. Zydney, Effect of solution pH and ionic strength on the separation of albumin from immunoglobulins (IgG) by selective ultrafiltration, Biotechnol. Bioeng. 43 (1994) 960–968.
[4] R.H.C.M. van Eijndhoven, S. Saksena, A.L. Zydney, Protein fractionation using electrostatic interactions in membrane filtration, Biotechnol. Bioeng. 48 (1995) 406–414.
[5] M. Feins, K.K. Sirkar, Novel internally staged ultrafiltration for protein purification, J. Membr. Sci. 248 (2005) 137–148.
[6] R. Ghosh, Novel cascade ultrafiltration configuration for continuous, high-resolution protein–protein fractionation: a simulation study, J. Membr. Sci. 226 (2003) 85–99.
[7] R. van Reis, A.L. Zydney, Bioprocess membrane technology, J. Membr. Sci. 297 (2007) 16–50.
[8] G.M. Rios, M.P. Belleville, D. Paolucci-Jeanjean, Membrane engineering in biotechnology: *quo vamus*? Trends Biotechnol. 25 (2007) 242–246.
[9] R.W. Field, D. Wu, J.A. Howell, B.B. Gupta, Critical flux concept for microfiltration fouling, J. Membr. Sci. 100 (1995) 259–272.
[10] J.A. Howell, Sub-critical flux operation of microfiltration, J. Membr. Sci. 107 (1995) 165–171.
[11] G.B. van den Berg, C.A. Smolders, Flux decline in ultrafiltration processes, Desalination 77 (1990) 101–133.
[12] R. Bowen, Understanding flux patterns in membrane processing of protein solution and suspensions, Trends Biotechnol. 11 (1993) 451–460.
[13] M. Hlavacek, F. Bouchet, Constant flowrate blocking laws and an example of their application to dead-end microfiltration of protein solutions, J. Membr. Sci. 82 (1993) 285–295.
[14] C.C. Ho, A.L. Zydney, A combined pore blockage and cake filtration model for protein fouling during microfiltration, J. Colloid Interface Sci. 232 (2000) 389–399.
[15] J. Hermia, Constant pressure blocking filtration laws: application to power-law non-Newtonian fluids, Trans. Inst. Chem. Eng. 60 (1982) 183–187.
[16] W.R. Bowen, J.I. Calvo, A. Hernandez, Steps of membrane blocking in flux decline during protein microfiltration, J. Membr. Sci. 55 (1991) 21–38.
[17] V. Lahoussine-Turcaud, M.R. Wiesner, J.Y. Bottero, Fouling in tangential-flow ultrafiltration: the effect of colloid size and coagulation pretreatment, J. Membr. Sci. 52 (1990) 173–190.
[18] B. Mehta, Processing of model compositional whey solutions with pressure driven membranes, Ph.D. Thesis, Ohio State University, 1973.
[19] M. Mondor, B. Girad, C. Moresoli, Modeling flux behavior for membrane filtration of apple juice, Food Res. Intern. 33 (2000) 539–548.
[20] P. Rai, C. Rai, G.C. Majumdar, S. DasGupta, S. De, Resistance in series model for ultrafiltration of mosambi (*Citrus sinensis Osbeck*) juice in a stirred continuous mode, J. Membr. Sci. 283 (2006) 116–122.
[21] G. Bolton, D. LaCasse, R. Kuriyel, Combined models of membrane fouling: development and application to microfiltration and ultrafiltration of biological fluids, J. Membr. Sci. 277 (2006) 75–84.
[22] C. Duclos-Orsello, W.Y. Li, C.C. Ho, A three mechanism model to describe fouling of microfiltration membranes, J. Membr. Sci. 280 (2006) 856–866.
[23] M. van Dyke, Perturbation Methods in Fluid Mechanics, Parabolic Press, Stanford, CA, 1975.
[24] R.G. Rice, D.D. Do, Applied Mathematics and Modeling for Chemical Engineers, Wiley, New York, 1995, pp. 195–207.
[25] S. Chellam, W.D. Xu, Blocking laws analysis of dead-end constant flux microfiltration of compressible cakes, J. Colloid Interface Sci. 301 (2006) 248–257.
[26] K.J. Hwang, C.Y. Liao, K.L. Tung, Analysis of particle fouling during mirofiltration by use of blocking models, J. Membr. Sci. 287 (2007) 287–293.
[27] S.T.D. de Barros, C.M.G. Andrade, E.S. Mendes, L. Peres, Study of fouling mechanism in pineapple juice clarification by ultrafiltration, J. Membr. Sci. 215 (2003) 213–224.